NeuroImage 240 (2021) 118299

Contents lists available at ScienceDirect

NeuroImage

journal homepage: www.elsevier.com/locate/neuroimage

Enhancing visual motion discrimination by desynchronizing bifocal oscillatory activity

Roberto F. SALAMANCA-GIRON[a,b], Estelle RAFFIN[a,b], Sarah B. ZANDVLIET[a,b], Martin SEEBER[c], Christoph M. MICHEL[c,g], Paul SAUSENG[d], Krystel R. HUXLIN[e], Friedhelm C. HUMMEL[a,b,f,*]

[a] *Defitech Chair in Clinical Neuroengineering, Center for Neuroprosthetics and Brain Mind Institute, Swiss Federal Institute of Technology (EPFL), Campus Biotech, Room H4.3.132.084, Chemin des Mines 9, Geneva, Switzerland*
[b] *Defitech Chair in Clinical Neuroengineering, Center for Neuroprosthetics and Brain Mind Institute, Clinique Romande de Readaptation (CRR), EPFL Valais, Sion, Switzerland*
[c] *Functional Brain Mapping Lab, Department of Fundamental Neurosciences, University of Geneva, Campus Biotech, Chemin des Mines 9, 1202, Geneva, Switzerland*
[d] *Department of Psychology, LMU Munich, Leopoldstr. 13, Munich 80802, Germany*
[e] *The Flaum Eye Institute and Center for Visual Science, University of Rochester, Rochester, NY, USA*
[f] *Clinical Neuroscience, University of Geneva Medical School, Geneva, Switzerland*
[g] *Lemanic Biomedical Imaging Centre (CIBM), Lausanne, Geneva, Switzerland*

ARTICLE INFO

Keywords:
Visual processing
Motion discrimination
Oscillatory synchronization
Noninvasive brain stimulation
Multisite tACS
Phase-amplitude coupling

ABSTRACT

Visual motion discrimination involves reciprocal interactions in the alpha band between the primary visual cortex (V1) and mediotemporal areas (V5/MT). We investigated whether modulating alpha phase synchronization using individualized multisite transcranial alternating current stimulation (tACS) over V5 and V1 regions would improve motion discrimination. We tested 3 groups of healthy subjects with the following conditions: (1) individualized *In-Phase* $V1_{alpha}$-$V5_{alpha}$ tACS (0° lag), (2) individualized *Anti-Phase* $V1_{alpha}$-$V5_{alpha}$ tACS (180° lag) and (3) *sham* tACS. Motion discrimination and EEG activity were recorded before, during and after tACS. Performance significantly improved in the *Anti-Phase* group compared to the *In-Phase* group 10 and 30 min after stimulation. This result was explained by decreases in bottom-up alpha-V1 gamma-V5 phase-amplitude coupling. One possible explanation of these results is that *Anti-Phase* $V1_{alpha}$-$V5_{alpha}$ tACS might impose an optimal phase lag between stimulation sites due to the inherent speed of wave propagation, hereby supporting optimized neuronal communication.

1. Introduction

Interactions among brain areas are assumed to be essential to most brain functions. Previous studies of inter-areal interactions have described the spiking activity of neurons in distant areas (Chouinard and Ivanowich, 2014; Nowak et al., 2008; Roe and Ts'o, 1999; Ruff and Cohen, 2016) under different contexts (Jia et al., 2013; Nowak et al., 2008; Oemisch et al., 2015; Pooresmaeili et al., 2014; Semedo et al., 2019). Neuroimaging studies in humans have also related specific connectivity patterns to behavioral profiles (Schipul et al., 2011; Wen et al., 2018), providing insight into how inter-regional interaction strength, directionality or spectral features are shaped by attentional state (Bosman et al., 2012; Oemisch et al., 2015; Ruff and Cohen, 2016), decision making (Gangopadhyay et al., 2021), stimulus drive (Jia et al., 2013; Roberts et al., 2013), or task demands (Pooresmaeili et al., 2014; Salazar et al., 2012).

The visual system is the archetype of a complex model that arises from the interplay among multiple brain regions that are hierarchically organized into a coarse, but richly interconnected network (Dosher and Lu, 1998; Gilbert et al., 2001; Gilbert and Sigman, 2007). For motion discrimination, research in humans (Blakemore and Campbell, 1969) and primates (Simoncelli and Heeger, 1998) has established that the primary visual cortex (V1) and medio-temporal areas (MT/V5, labeled henceforth as V5) are co-activated in complementary feedforward and feedback sweeps (Lamme and Roelfsema, 2000; Newsome and Pare, 1988), sweeps that are tuned to the characteristics of the stimulus (e.g., orientation) and to the anatomical pathways that are recruited. Moreover, this channel is endowed with specific patterning of electrical signals. Recent evidence suggests that communication between these two regions may be established by orchestrated phase synchronization of oscillations at lower frequencies (i.e., at Alpha-Beta frequencies, <25 Hz), acting as a temporal reference frame for information conveyed by high-

* Corresponding author at: Defitech Chair in Clinical Neuroengineering, Center for Neuroprosthetics and Brain Mind Institute, Swiss Federal Institute of Technology (EPFL), Campus Biotech, Room H4.3.132.084, Chemin des Mines 9, Geneva, Switzerland.
E-mail address: friedhelm.hummel@epfl.ch (F.C. HUMMEL).

https://doi.org/10.1016/j.neuroimage.2021.118299.
Received 16 February 2021; Received in revised form 11 June 2021; Accepted 20 June 2021
Available online 22 June 2021.

frequency activity (at Gamma frequencies >40 Hz) (Bastos et al., 2015; Bonnefond et al., 2017; Fries, 2009; Seymour et al., 2019). In fact, the orchestrated interactions between Alpha and Gamma oscillations may serve as a framework supporting the feedforward and feedback loops of inter-regional brain communication within the visual system (Kerkoerle et al., 2014; Michalareas et al., 2016). Specifically, top-down Alpha appears to control the timing and elicitation of higher frequency rhythms, thus optimizing communication in the visual cortex (Fries, 2015; Michalareas et al., 2016).

More generally, phase synchronization is a key neuronal mechanism that drives spontaneous communication among dynamical nodes (Gollo et al., 2014), implying that this mechanism supports attentional, executive, and contextual functions (Doesburg et al., 2009; Freunberger et al., 2007; Palva and Palva, 2011). The two simplest phase synchronization patterns are *in-phase synchronization* (i.e., zero phase lag between the two regions) and *anti-phase synchronization* (i.e., 180° phase lag between the two regions). In-phase synchronization between two distant neuronal populations is thought to serve the integration of separated functions that are performed in these different regions (Engel et al., 1991; Roelfsema et al., 1997; Wang et al., 2010). Conversely, anti-phase patterns reflect more dynamical reciprocity, where certain areas of the brain increase their activity while others decrease their own activity. Such anti-phase patterns have been reported during sleep (Horovitz et al., 2009), or during visual attentional tasks (Yaple and Vakhrushev, 2018). It has been proposed that these anti-phase oscillation patterns reflect time-delays in functional coupling between two connected regions (Petkoski and Jirsa, 2019). Since communication between neurons is achieved by propagation of action potentials throughout axons, with conduction times defined by some regional specificities, such as myelination density, number of synaptic relays, inhibitory couplings etc., an optimal phase delay relationship between two interconnected regions could be a key driver of successful brain communication.

In this article, we set out to determine whether motion discrimination performance can be enhanced when 'artificially' entraining/manipulating the phase relationship between V1 and V5. This is based on the idea that inter-areal synchronization plays a significant role in V1-V5 communication, as demonstrated previously (Lewis et al., 2016; Siegel et al., 2008). We used individually adjusted, Alpha transcranial alternating current stimulation (tACS) to entrain endogenous oscillations (Helfrich et al., 2014) and enhance inter-areal information flow (Zhang et al., 2019). The modulation consisted in applying approximately 15 min of concurrent, bifocal (over V1 and V5), individualized Alpha-tACS. We assessed two conditions of stimulation: In-Phase (zero phase lag) stimulation and Anti-Phase stimulation (180° phase lag); and a Sham tACS group was evaluated to control for non-specific, placebo-like effects.

Furthermore, the entire experiment was conducted while recording multi-channel electroencephalography (EEG). Electrophysiological analyses were computed with the objective of determining EEG markers of interareal modulation between the two target areas. We paid special attention to connectivity metrics in the Alpha band, as well as in the Gamma band because of their role in visual feature binding (Elliott and Müller, 1998; Gray and Singer, 1989; Zhang et al., 2019) and inter-areal communication in the visual cortex (Fries, 2015; Michalareas et al., 2016). Taken together, we hypothesize that the best inter-areal Alpha phase relationship for optimal oscillatory entrainment leading to respective behavioral enhancement is associated with changes in Alpha-Gamma coupling within the V1-V5 pathway.

2. Materials and methods

2.1. Subjects

50 healthy subjects were recruited (range age: 18 to 40 years old, 24 females). All individuals were right-handed with normal or corrected to normal vision, and had no history of neurological diseases or cognitive disability. A written consent form was obtained from all participants prior the experiment. The study was performed according to the guidelines of the Declaration of Helsinki and approved by the local Swiss Ethics Committee (2017–01,761).

2.2. Study design

Individual testing started with a familiarization phase followed by the actual experiment. During the familiarization phase, we ensured that the subject understood the visual discrimination task and reached stable performance. After EEG acquisition was prepared, a baseline block, which consisted of a task-related EEG recording without tACS was started. After a few minutes of rest, electrodes were placed over the occipital and temporal cortex, and electrical stimulation was started, remaining on for the entire duration of the block. Immediately after the start of stimulation, the second timepoint (TP0) was recorded with concurrently-measured EEG. Thereafter, the stimulation electrodes were removed and after a few minutes of rest, two succeeding evaluation points (TP10: 10 min after stimulation, TP30: 30 min after stimulation) were measured using the same task-related EEG setup, without tACS (see **Fig. 1A**).

2.3. Visual discrimination task

The visual task used is a well-established 2-alternatives, forced-choice, left-right, global direction discrimination and integration task (150 trials per time point) (Das et al., 2014; Huxlin et al., 2009). The stimulus consisted of a group of black dots moving globally left- or rightwards on a mid-gray background LCD projector (1024 × 768 Hz, 144 Hz) at a density of 2.6 dots per degree and in a 5° diameter circular aperture centered at cartesian coordinates [−5°, 5°] (i.e., the bottom left quadrant of the visual field, relative to central fixation) (see Fig. 1B and 1C). This stimulus location was used to optimized V5 activation strength based on previous literature (e.g., (Albright, 1989); (Seiffert et al., 2003)). Direction range of the dots was varied between 0° (total coherence) and 360° (complete random motion). The degree of difficulty was increased with improving task performance by increasing the range of dot directions within the stimulus. A 3:1 staircase design was implemented to allow us to compute a threshold level of performance for direction integration at the end of each timepoint (Das et al., 2014; Huxlin et al., 2009). For every 3 consecutive correct trials, direction range increased by 40°, while for every incorrect response, it decreased by 40°. The black dots making up the stimulus were 0.06° in diameter and moved at a speed of 10° per second over a time lapse of 250 ms for a stimulus lifespan of 500 ms. At every stimulus onset, an auditory beep was played for the subject. After each trial, auditory feedback indicated whether the response was correct or incorrect. Correct trials were followed by two beeps at 800 Hz and 1000 Hz. Incorrect trials were followed by two beeps at 500 Hz and 400 Hz.

2.4. Transcranial electrical stimulation

Subjects were randomly assigned into 3 groups: In the first experimental group (n = 17, 10 females), In-Phase (0° phase lag) bifocal tACS was applied over the right V1 and V5 areas. The second experimental group (n = 18, 8 females), received Anti-Phase (180° phase lag) bifocal tACS over V1 and V5 areas, also in the right hemisphere (see Fig. 1E). The control group (n = 15, 6 females) received Sham (i.e., ramp up and subsequent ramp down lasting in total one individually defined alpha cycle) bifocal stimulation over identical V1 and V5 locations as the first two groups. The electrode placement on V1 and V5 were determined according to the 10–20 EEG system, based on previous literature investigating motion processing (Kar and Krekelberg, 2014)(Michalareas et al., 2016) (Hülsdünker et al., 2019) (Zito et al., 2015) i.e., covering the Oz-

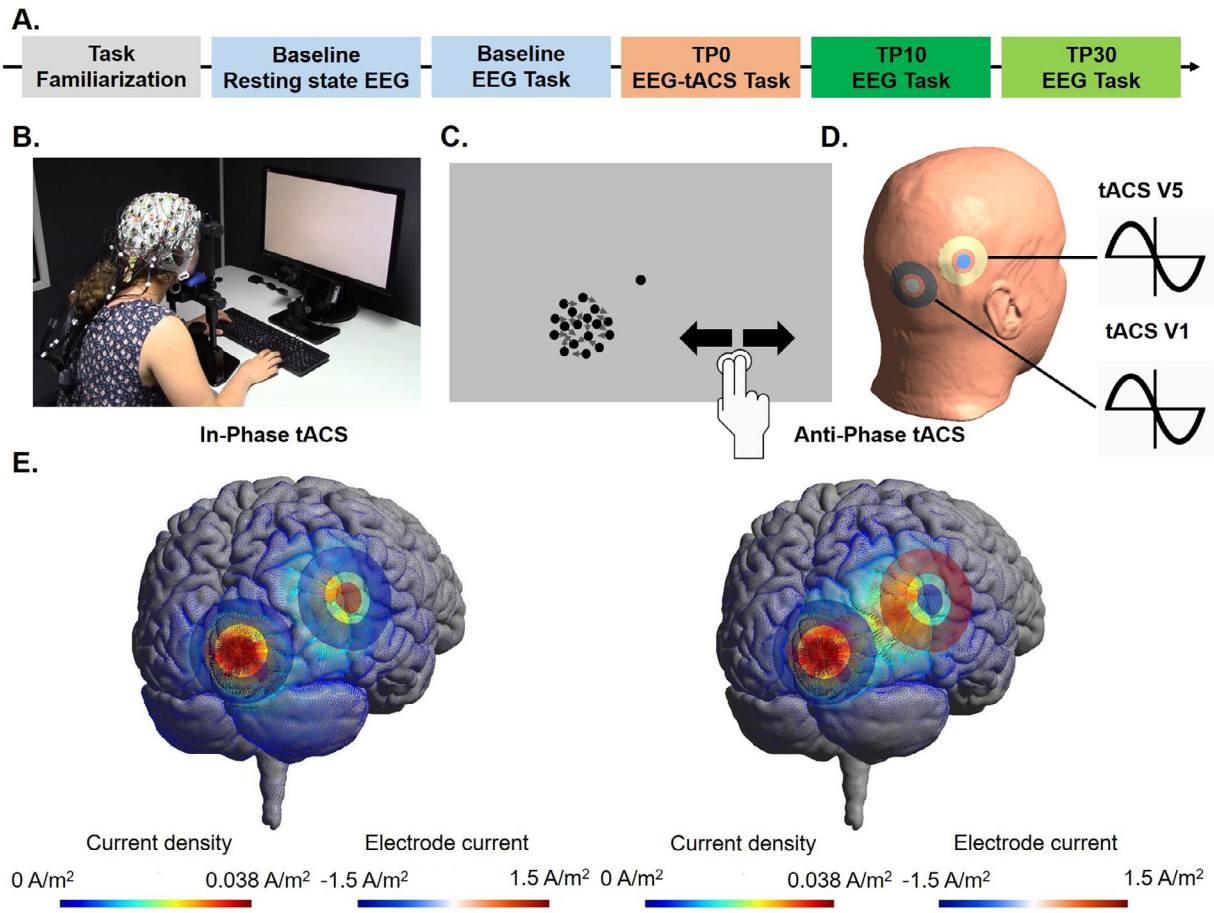

Fig. 1. General features of the study (A) Experimental design. The total duration of the experiment was around 3 hrs. **(B) Real example** of the experimental setup inside the Faraday's cage. The EEG system and an ongoing visual task are shown. **(B) Schematic example of the motion discrimination task. (C) Schematic of the bifocal tACS** applied with concentric electrodes over P6 and O2 while subject performs the global direction discrimination visual task. (**D) Electrical field 3D representation of bifocal tACS** at the two different phase differences (Thielscher et al., 2015). The dispersion of the field does not change over time in the two conditions, but rather the magnitude of the electrical field lines (Saturnino et al., 2017).

O2 and P08-P6 electrodes, respectively. Fig. 1D gives an overview on the stimulating electrodes' positions for the three groups.

Prior to the baseline recording, the Alpha peak frequency of each individual was determined over a 180s-long EEG resting-state recording with the eyes open, used thereafter as the individualized frequency for the tACS in time point TP0. The individualization of the Alpha rhythm is justified by the idea that Alpha rhythms appear to be in charge of bottom-up and top-down inter areal sweeps, that ultimately gate and time the information flow in cortical networks (Sauseng et al., 2009; von Stein et al., 2000). Moreover, there have been several examples of non-invasive stimulation studies showing that tailoring the oscillatory traces to the endogenous Alpha rhythms, effectively modulates the ongoing activity (Neuling et al., 2013; Vosskuhl et al., 2016; Zaehle et al., 2010). Mean Alpha stimulation frequency for the In-Phase group was 9 Hz (range 7–11 Hz), for the Anti-Phase group:10 Hz (range 7–12 Hz) and for the Sham group: 10 Hz (range 7–11 Hz).

2.5. Apparatus and devices

All experiments took place inside the same, shielded Faraday cage designed for EEG recordings, and under the same light conditions. Participants' heads were placed over a chin-rest at a distance of 60 cm from the presentation screen, assuring a fixed position across all trials. The task ran on a Windows OS machine, based on a custom Matlab (The MathWorks Inc., USA) script, using the Psychophysics Toolbox.

Gaze and pupils' movements were controlled in real time with an EyeLink 1000 Plus Eye Tracking System (SR Research Ltd., Canada) sampling at a frequency of 1000 Hz. The task required the subject to fixate a target at the center of the screen for every trial, with a maximal tolerance for eye deviation from this fixation target of about 1°. If the participant broke fixation during stimulus presentation, the moving stimulus froze and then disappeared; the trial was discontinued, and an auditory tone (at 400 Hz) was presented. Once the participant repositioned their gaze correctly, a novel trial was started.

Bifocal tACS was delivered by means of two Neuroconn DC Plus stimulators (Neurocare group) triggered every cycle repeatedly to assure the chosen phase synchronization between the two stimulation sites. Custom-made, concentric, rubber electrodes of external diameter 5 cm, internal diameter of 1.5 cm and 2.5 cm of hole diameter were used to deliver stimulation. The intensity was fixed to 3 mA corresponding to a current density of 0.18 mA per cm^2. The electrodes were held by placing the EEG cap over them. The period of continuous stimulation, although it was slightly different for every participant, took on average ~13 ± 2 min (SEM), i.e., the time to complete 150 trials of the motion discrimination task described above. The inter-individual variability in the stimulation duration is explained by the fact that participants were told to be as accurate as possible without having any time pressure, resulting in a relatively large inter-individual variability in reaction times, hence durations to complete the 150 trials.

EEG was recorded from a 64 channels passive system (Brain Products GMBH) at a sampling frequency of 5 kHz.

2.6. Data analysis

Behavioral data: For each subject and time point, we extracted direction range thresholds using all trials, by fitting a Weibull function, which defined the direction range level at which performance reached 75% correct. These direction range thresholds were then normalized to the maximum possible range of motion (360°), resulting in a normalized direction range threshold (NDR), a procedure previously described (Das et al., 2014; Huxlin et al., 2009).

$$NDRthreshold(\%) = \left[\frac{(360° - Weibull fitted DR)°}{360}\right] * 100$$

Finally, NDR thresholds were corrected for inter-individual variability in baseline performances by dividing all data by the individual baseline performances (referred as baseline-corrected NDR throughout the manuscript).

EEG data: All analyses on EEG data were performed on periods without tACS (at Baseline, TP10 and TP30) using MNE-Python (Gramfort et al., 2013) and customized scripts.

For the preprocessing, data were re-referenced to the average of signals, filtered through a Finite Response Filter of order 1, between 0.5 and 45 Hz, epoched in 3 s blocks, corresponding to −1.5 s before and +1.5 s after the stimulus onset. Every epoch corresponded to the time interval of a trial from the behavioral task. They were visually inspected to clear up noisy channels or unreadable trials. Bad channels were interpolated, data was re-sampled to 250 Hz. Independent component analysis was used to remove physiological artifacts (i.e., eyeblinks, muscle torches).

For analyses in the frequency domain, Morlet wavelets convolution changing as a function of frequency was applied to 40 frequency bins, between 2 and 42 Hz, increasing logarithmically.

For the source reconstruction analyses, data was re-referenced to the average of signals, noise covariance matrix was calculated to enhance the source approximation, a template brain and segmentation was used to compute the forward solution for 4098 sources per hemisphere. The inverse solution was calculated by means of MNE algorithm (Hämäläinen and Ilmoniemi, 1994). The source estimates were computed with dipole orientations perpendicular to the cortical surface (Lin et al., 2006). The source points belonging to specific areas of interest (i.e. V1 and V5), were defined using the templates provided in the "SPM" open access database included in the MNE library (Wakeman and Henson, 2015). In order to extract one time-series per area of interest, we computed the first principal component from all source dipoles within each area. This first principal component is representing the source estimates associated with these pre-defined areas. Subsequently, a sign-flip was applied with the objective of avoiding sign ambiguities in the phase of different source estimates within the same area (Gramfort et al., 2012).

From the preprocessed EEG signals, we extracted a series of markers to depict the global features of the signal in the temporal, spectral and spatial domains with a specific focus on the activity over V1 and V5 and the coupling between the two areas, in the two frequency bands of interest: Alpha and Gamma rhythms. Specifically, the EEG metrics of interest computed were: Power Spectral Density (PSD) in the Alpha and Gamma band, both computed in the sensors' space, Coherence and Imaginary Coherence in the Alpha and Gamma Band, V1 Alpha Phase to V5 Gamma Amplitude coupling (ZPAC-V1pV5a) and, V5 Alpha Phase to V1 Gamma Amplitude coupling (ZPAC-V5pV1a), computed in the sources' space. Given that the sensor signals have passed through a source reconstruction method prior the calculation of the connectivity metrics, the problem of volume conduction is reduced (Hoechstetter et al., 2004). All these variables were baseline-normalized. Moreover, the Phase Amplitude coupling (i.e. PAC) was standardized to avoid confounders by creating a non-parametrized distribution of values to which to compare the observations through a Z-score transformation (i.e. ZPAC) (Canolty et al., 2006; Cohen, 2014).

Thus, PSD (Φ) was calculated taking an average of all electrodes through the Welch's estimator (Welch, 1967), that considers averaging PSDs from different windows, according to the formula:

$$\Phi(f) = \frac{1}{K}\sum_{i=1}^{K}\frac{1}{W}\left|X_K(v)\right|^2, whereW = \sum_{m=1}^{M} w^2[m]$$

Where K corresponds to the number of segments where a windowed Discret Fourier Transform is computed, X is the segment where it is computed at some frequency v and w is the window segment

(Magnitude-square) Coherence (Carter, 1987) was calculated through:

$$C_{xy}(f) = \frac{\left|\Phi_{xy}(f)\right|^2}{\Phi_{xx}(f)\cdot\Phi_{yy}(f)}$$

V1-V5 coherence analyses are used to investigate frequency-specific phase coupling between these source areas. Although coherence values might be biased due to source leakage effects (Palva et al., 2018), we included this metric because it is of relevance given our brain stimulation approach. Specifically, we expect that tACS will modulate the amplitude of the endogenous the Alpha, fact that will have direct repercussions in the weighting of the (Magnitude Square) Coherence metric.

Imaginary Coherence (Nolte et al. 2014), followed the formula:

$$IC_{xy}(f) = \frac{I\left[\Phi_{xy}(f)\right]}{\sqrt{\Phi_{xx}(f)\cdot\Phi_{yy}(f)}}$$

Where I denotes the imaginary part of the numerator. Although we do not expect this metric to directly catch changes in the Alpha amplitude modulated by the tACS, the Imaginary Coherence was chosen as a connectivity metric that is not influenced by volume conductance

Phase Amplitude coupling (PAC) (Canolty et al., 2006) was obtained through:

$$PAC = n^{-1}\sum_{t=1}^{n} a_t(f)\cdot e^{i\theta t}\vee$$

Where t corresponds to a certain time point, a denotes the power at a certain specific frequency for this specific time point, i is the imaginary variable, θ the phase angle and n the number of time points. PAC values were Z-transformed (i.e., ZPAC) by means of a non-parametric permutation test. This was carried out by shuffling repeatedly the power values (maintaining the phase array) with the aim of drawing a distribution allowing null hypothesis testing. This distribution was then used to make a comparison with every observation. Ultimately, this procedure avoids problems of circular normality, power fluctuations and scaling (Cohen, 2014). In the manuscript, we will refer to ZPAC V1 Alpha phase – V5 Gamma amplitude (ZPAC-V1p_{Alpha}V5a_{Gamma}) as a bottom-up modulation and PAC V1 Gamma amplitude – V5 Alpha phase (ZPAC-V1a_{Gamma}V5p_{Alpha}) as a top-down modulation (see Nandi et al., 2019). We have chosen a priori these two bands of interest, Alpha and Gamma, because the oscillatory traces that have been widely reported in literature of the visual system rather correspond to these two frequency bands (Michalareas et al., 2016; (van Kerkoerle et al., 2014) (Doesburg et al., 2009); Fries, 2015; Gray and Singer, 1989; Hanslmayr et al., 2011; Jensen and Mazaheri, 2010; Michalareas et al., 2016; Tu et al., 2016). Moreover, our hypothesis is built under the premise that if we stimulate in the Alpha band, that is the frequency that is going to be modulated (Dosher and Lu, 1998) by the stimulation. In order to verify the lack of influence concerning the signal leakage problem in the calculation of the Phase Amplitude Coupling, computations showing the modulation of the phase and amplitude within the same areas of source estimates were computed (See supplementary Fig. 2).

2.7. Statistical analyses

Behavior: Statistical analyses were carried out using mixed-effect linear models. The evolution of the baseline-corrected NDR was investi-

gated as a dependent variable, with stimulation group and time points as the main fixed effects.

EEG metrics: PSD (Gamma and Alpha components across time) significance within subjects was tested through a sliding FDR-corrected T-test. Significance within subjects in the Coherence and Phase-Amplitude coupling spectrums were evaluated through non-parametric permutation tests and clusters-based corrected for multiple comparisons. Differences were considered significant when $p < 0.05$.

A mixed linear model was performed in order to evaluate the variability of the chosen EEG metric (dependent variable) over time, among stimulation groups.

Best EEG metric: In order to determine the EEG metric that had the highest impact on the behavioral scores and then reduce the model space of the baseline-corrected NDR mixed linear model, an embedded regularization method (i.e., least absolute shrinkage and selection operator - Lasso) was applied (Tibshirani, 1996) following the Langragian version of the formula:

$$argmin_{\beta}\|y - F \cdot \beta\|^2 + \lambda_s\|\beta\|$$

Where β corresponds to the unknown vector of weighted coefficients estimated for every metric (regression coefficient), y is the matrix with all the labeled metrics, λ is in charge of the variable selection and F correspond to the acquired data points. Lasso was selected due to the fact that it provides a preferred solution with the highest sparsity given the shrink provided by the penalty term. The vector of λ chosen consisted in 30 testing points spaced between 0 and 1. The number of iterations was set to 1000.

Behavior ± EEG: As a second step, covariates that could explain variance in NDR outcome and a possible interaction effect with stimulation group were added to the first mixed linear model. A random intercept per subject was used to correct for the dependency between time points for all models. Given that we implement a single mixed linear model with several factors accounting for the variance of the same variable (i.e., NDR), there is no need to correct for multiple comparisons. All contrasts were obtained by changing the labels at the intercept. The residuals of each statistical model were tested for normality by inspecting histograms and through the omnibus normality test (D'Agostino and Pearson, 1973).

3. Results

All participants tolerated the stimulation well and did not report any adverse effects, such as peripheral sensory or phosphene perception. Five participants could not be included in the analyses: One participant discontinued the experiment without stating the reason for it and four participants were discarded, due to poor performance (60% correct responses or less). Poor task performance prevented reliable curve-fitting procedures to extract our primary output, the direction range thresholds. Therefore, 45 full sets of data were analyzed, forming homogeneous groups of 15 participants/group. For the EEG metrics of interest (ZPAC), three data points (i.e., 2 from the In-Phase group, 1 from the Anti-Phase group) were found by Cook's Distance algorithm (Cook, 1977) to be more than two standard deviations from the mean of the distribution, and were thus not included in the analyses.

3.1. Motion direction performance throughout groups and time

Fig. 2A displays the mean baseline-corrected NDR thresholds across participants, reflecting the normalized motion direction value corresponding to 75% correct performance (see Method section) across groups and time. There was no statistically significant difference between groups at baseline (Anti Phase vs. In Phase $b = 1.670$, $P = 0.809$, CI = −11.835 15.175, Sham vs. In Phase $b = 3.260$, $P = 0.624$, CI = −9.770 16.290, Sham vs Anti Phase $b = 1.590$, $P = 0.815$, CI = −11.696 14.876; see also Supplementary Table 1 providing the raw NDR values), as the baseline values showed large variability, we applied a baseline correction procedure to account for this variability. When considering all the groups together, the change in baseline-corrected NDR was not significant between TP0 and TP10 ($b = -0.05$, $P = 0.189$, CI = −0.124 0.024) nor between TP0 and TP30 ($b = -0.067$, $P = 0.079$, CI = −0.141 0.008), neither between TP10 and TP30 ($b = -0.017$, $P = 0.657$, CI = −0.091 0.057). However, there was a significant difference at TP0, TP10 and TP30 between the In-Phase and the Anti-Phase group ($b = 0.257$, $P = 0.015$, CI = 0.05 0.464). There was no difference for other group comparisons for all time points ($b = 0.16$, $P = 0.118$, CI = −0.04 0.36 Sham and In-Phase; $b = -0.097$, $P = 0.349$, CI = −0.301 0.107 Sham and Anti-Phase).

3.2. EEG results

In all participants, the visual discrimination task led to an amplitude increase in the Theta/Low Alpha band, right after the onset of the stimulus, followed by a phasic decrease in power in the High Alpha/Low Beta bands ~200 ms thereafter (**Fig. 2B**). Additionally, in frequencies above 30 Hz, there was a constant decrease in magnitude during stimulus presentation, as previously described in the literature for this type of visual task (e.g., Siegel et al., 2007; Townsend et al., 2017).

The Lasso model, defined for each time point, showed that a single EEG marker, namely ZPAC-V1p_{Alpha}V5a_{Gamma} had the largest explanatory value for the variance of NDR at TP10 (R^2=0.1081, λ=0.0516) and TP30 (R^2=0.0731, λ=0.1114), irrespective of the stimulation group.

Since the ZPAC-V1p_{Alpha}V5a_{Gamma} values best explained changes in the performance after stimulation, the rest of the manuscript focuses on this metric in order to further explore stimulation and time effects. The opposite direction, ZPAC-V1a_{Gamma}V5p_{Alpha} was used as a control analysis to test for the directional specificity of the present results.

Changes in bottom-up V1 Alpha phase (V1p_{Alpha}) - V5 Gamma amplitude (V5a_{Gamma}) coupling

Fig. 3A shows the mean baseline-corrected ZPAC-V1p_{Alpha}V5a_{Gamma} values for the three groups across time. As a pre-requisite, we ensured that there was no significant difference at baseline between the In Phase group and the Anti Phase group ($b = -0.506$, $P = 0.486$, CI = −1.93 0.918) nor between the In Phase and the Sham group ($b = -1.052$, $P = 0.121$, CI = −2.382 0.279). Likewise, there was no significant difference between the Anti Phase and the Sham group ($b = -0.545$, $P = 0.422$, CI = −1.878 0.787). These values were extracted from the significant modulation of interest between the Alpha/High Theta and the Low Gamma bands shown in Fig. 3B. It reveals a significant diminishment in the Alpha/High Theta (5–12 Hz) – Low Gamma (30–42 Hz) phase amplitude coupling at TP10 for the Anti-Phase and the Sham group and a significant augmentation in coupling for the In-Phase group. At TP30, there is overall a more prominent augmentation of the coupling for the In-Phase group, a more pronounced diminishment for the Anti-Phase and rather a stable response for the Sham group. To statistically analyze the descriptive differences between the three conditions, we computed a mixed linear model on the ZPAC-V1p_{Alpha}V5a_{Gamma}values. The model returned a marginally significant change over time between the interval TP10 and TP30 ($b = -0.769$, $P = 0.055$, CI = −1.556, 0.018), but no significant differences between the Anti-Phase and the In-Phase groups ($b = 0.836$, $P = 0.35$, CI =−0.916, 2.588). This held true also when comparing the Anti-Phase and Sham groups ($b = 1.009$, $P = 0.249$, CI = −0.708 2.726), and the In-Phase and Sham groups ($b = 0.173$, $P = 0.84$, CI = −1.51 1.856).

When ZPAC-V1p_{Alpha}V5a_{Gamma}values were entered as a single confounder into the baseline-corrected NDR model, it did not significantly account for the overall variance for all the stimulation groups at all time points ($b = 0.015$, $P = 0.196$, CI = −0.008, 0.039). However, ZPAC-V1pV5a from the Anti-Phase group as compared to the In-Phase group, did significantly account for the variability of the NDR as a fixed effect over time at both TP10 and TP30 ($b = 0.071$, $P = 0.048$, CI = 0.001,

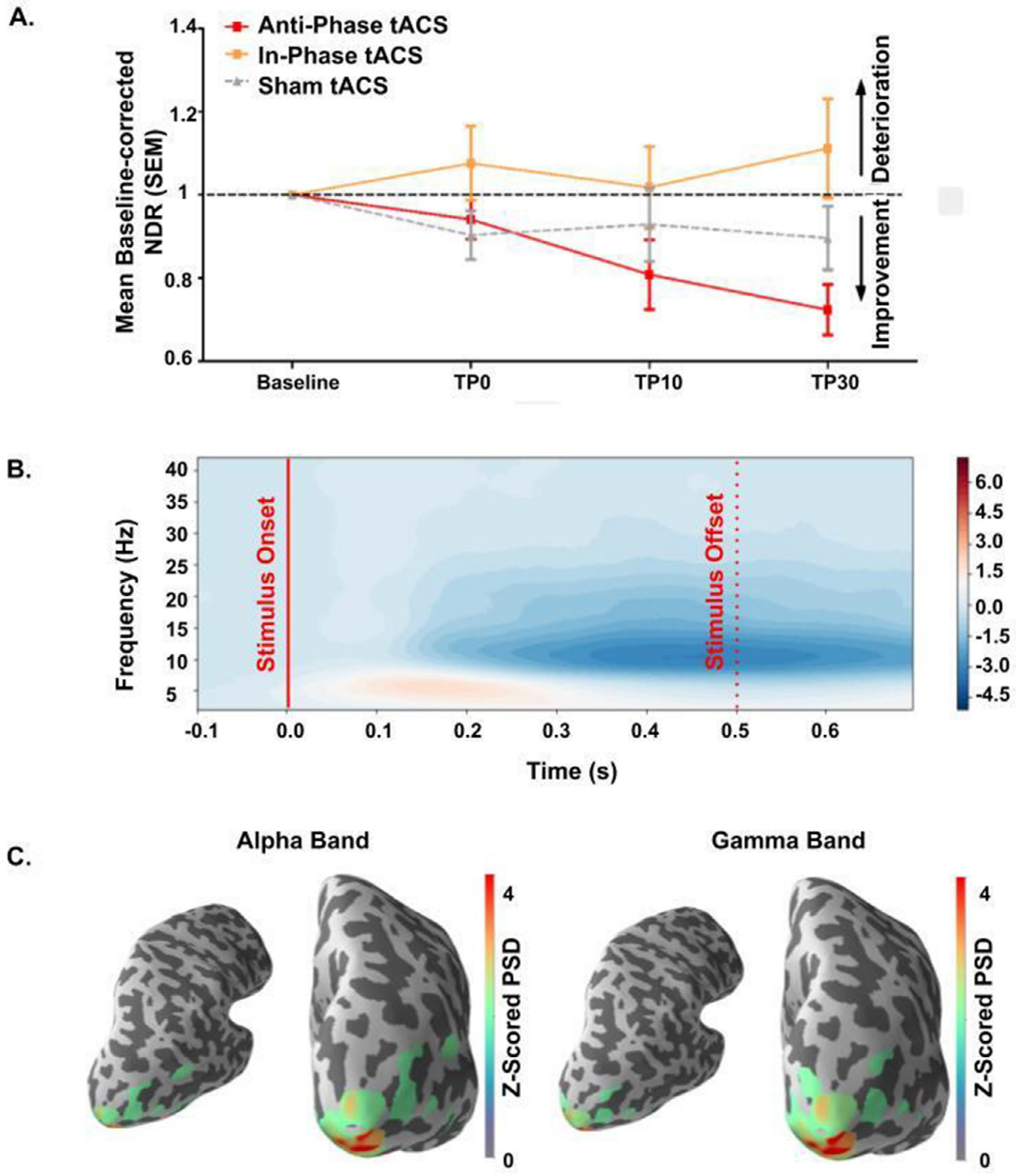

Fig. 2. Main behavioral results and their main EEG associated traces. (A) Baseline-corrected NDR (Normalized Direction Range) threshold evolution across time-points for the three stimulation conditions. Bars correspond to Standard Errors of the Mean (SEM). Anti-Phase stimulation induced an increased performance translating into a significantly pronounced behavioral improvement over time at the group level. The behavioral performance of the Anti-Phase group was significantly enhanced compared to the In-Phase group. **(B) Time-frequency representation** of the averaged response during a trial at the baseline period, before the stimulation. It shows a typical Event Related Synchronization at (ERS) the Theta/Alpha band, followed by an Event Related Desynchronization (ERD) in the Beta band (in z-scores). **(C)** 3D plot representation of the normalized activation of sources V1 and V5 of interest defined using the templates provided in the "SPM" open access database included in the MNE library (Wakeman and Henson, 2015) for the Alpha and Gamma band during the stimulus presentation.

0.142). This was not the case when comparing the ZPAC-V1pV5a values from the In-Phase group versus those from Sham ($b = -0.023$, $P = 0.44$, CI = 0.081, 0.035), nor when comparing those from Anti-Phase and Sham groups ($b = 0.048$, $P = 0.095$, CI = −0.008, 0.105) at any of the two time points (all other comparisons are shown in the Supplementary Table 2).

3.3. Changes in top-down V1 gamma amplitude ($V1a_{Gamma}$) - V5 Alpha phase ($V5p_{Alpha}$) coupling

To test the eventual directional specificity of the present results, we examined the opposite phase-amplitude coupling between V1 and V5. **Fig. 4A** provides the descriptive data for the ZPAC-$V1a_{Gamma}V5p_{Alpha}$

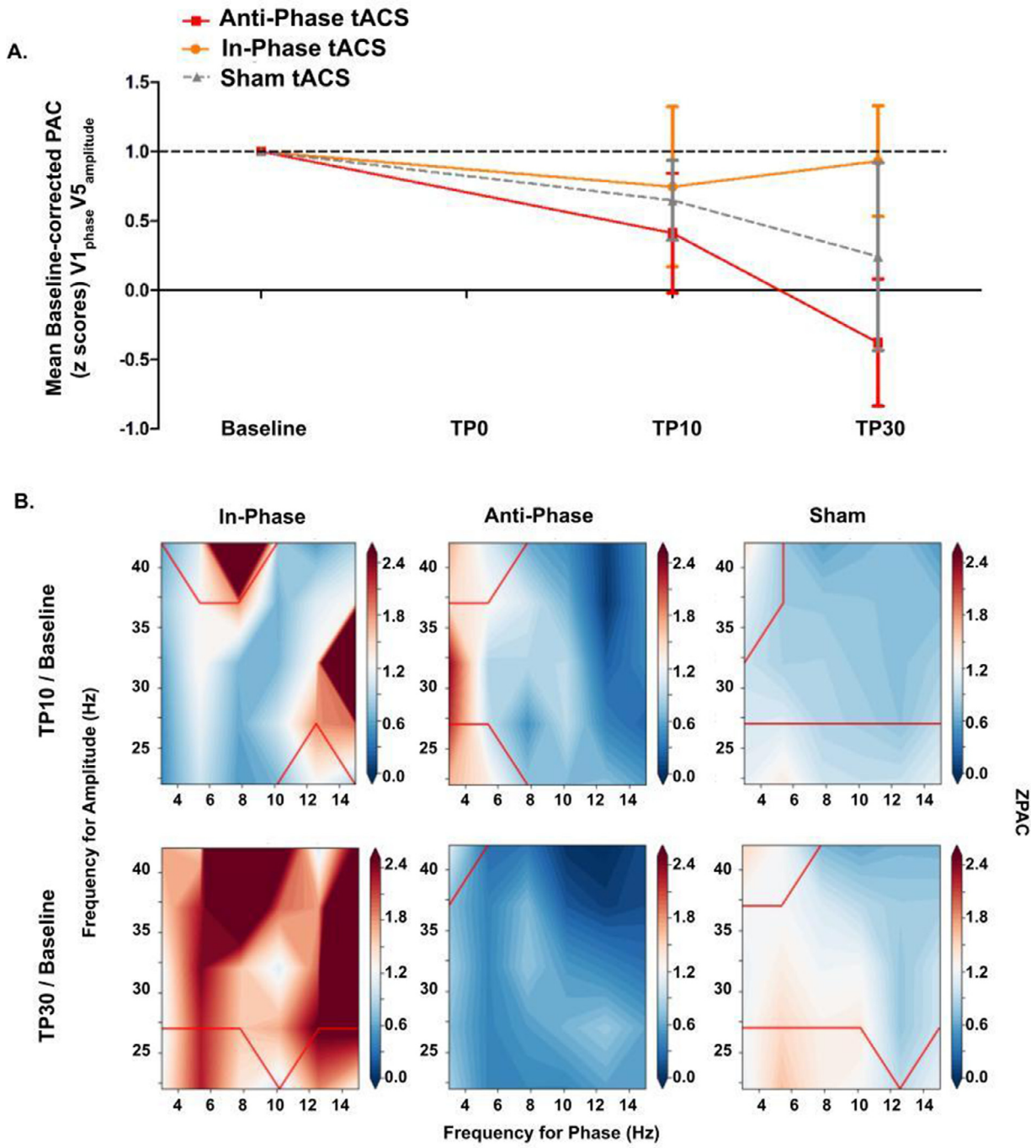

Fig. 3. V1-Alpha phase V5-Gamma Amplitude PAC (A) Baseline-corrected, bottom-up V1-Alpha phase V5-Gamma Amplitude coupling across time-points. Bars correspond to Standard Errors of the Mean (SEM). Please note the strong decrease for the In-Phase group towards TP30. (**B) Averaged, baseline-corrected, V1-Gamma amplitude V5-Alpha phase coupling spectrums** for the three stimulation groups and for the two time points after stimulation averaged during the stimulus presentation interval. Significant clusters are highlighted in red ($p<0.05$, corrected for multiple comparisons).

for all 3 experimental groups over time. To statistically analyze these data, we applied a comparable approach as in the previous section. Baseline comparison revealed no overall baseline difference group versus Anti-Phase group ($b = -0.587$, $P = 0.457$, CI = −2.136 0.962), In-Phase group versus Sham group ($b = 0.141$, $P = 0.85$, CI = −1.318 1.599) and Anti Phase group versus Sham group ($b = 0.728$, $P = 0.324$, CI = −0.718 2.175). Fig. 4**B** shows the results for the ZPAC-V1a$_{Gamma}$V5p$_{Alpha}$, which appeared to have a significant Alpha/Theta – Low Gamma phase amplitude cluster at both TP10 and TP30. Diminished coupling is evident for the three stimulation groups when V5 Alpha/ High Theta (6–10 Hz) modulated Low V1 Low Gamma (30–37 Hz) amplitude. We then built a similar mixed linear model using the ZPAC-V1a$_{Gamma}$V5p$_{Alpha}$ values. These analyses showed no significant change in time between TP10 and TP30 ($b = 0.409$, $P = 0.286$, CI = −0.343, 1.161). Neither at TP10 nor at TP30 was a significant difference between the Anti-Phase and Sham group ($b = -0.718$, $P = 0.484$, CI = −2.727, 1.292), between

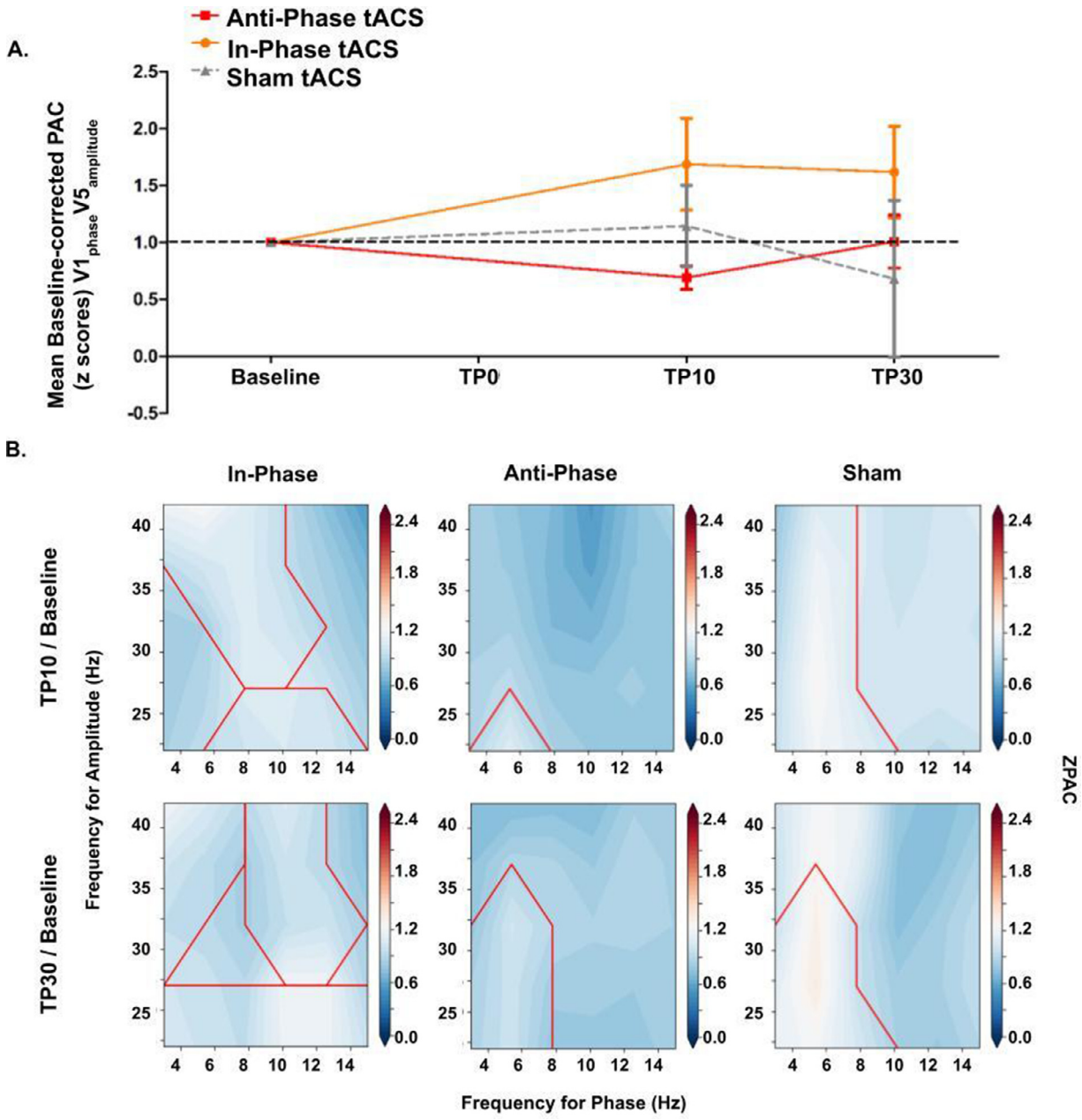

Fig. 4. V1-Gamma amplitude V5-Alpha phase PAC (A) Baseline-corrected, top-down V1-Gamma amplitude V5-Alpha phase coupling across time-points. Bars correspond to Standard Errors of the Mean (SEM). **(B) Averaged, baseline-corrected, V1-Gamma amplitude V5-Alpha phase coupling spectrums** for the three stimulation groups and for the two time points after stimulation averaged during the stimulus presentation interval. Significant clusters are highlighted in red (p<0.05, corrected for multiple comparisons).

the Anti-Phase and In-Phase group (b = 0.695, P = 0.506, CI = −1.353, 2.744) or between the In-Phase and Sham group (b = −1.413, P = 0.161, CI = −3.39, 0.564). Unsurprisingly, when ZPAC-V1a$_{Gamma}$V5p$_{Alpha}$ was entered as a confounder into the NDR model, it did not significantly account for the variance in NDR scores for all the stimulation groups together at all time points (b = −0.007, P = 0.53, CI = −0.029, 0.015). Additionally, there was an absence of a significant interaction between ZPAC-V1a$_{Gamma}$V5p$_{Alpha}$ and each stimulation group, suggesting that the ZPAC-V1a$_{Gamma}$V5p$_{Alpha}$ group values did not explain the group differences in the NDR values at all timepoints (In-Phase vs. Anti-Phase: b = −0.055, P = 0.432, CI = −0.191, 0.082, In-Phase vs. Sham: b = 0.006, P = 0.908, CI = −0.09, 0.101, Anti-Phase vs. Sham: b = 0.06, P = 0.234, CI = −0.039, 0.16) (all other comparisons are shown in the Supplementary Table 3).

4. Discussion

By applying multisite tACS in the Alpha range to V1 and V5 with a phase difference of 180° (Anti-Phase) with respect to zero degree (In-Phase), we were able to improve motion direction discrimination and integration in young healthy individuals, by modulating inter-regional oscillatory coupling between the two stimulated areas (see Fig. 5). More specifically, the three main findings can be summarized as follows: (1) *Anti-Phase* V1$_{Alpha}$-V5$_{Alpha}$ tACS stimulation leads to an improvement in visual performance shortly after stimulation compared to *In-Phase* V1$_{Alpha}$-V5$_{Alpha}$, which appears rather detrimental to motion discrimination and integration, (2) improved performance with *Anti-Phase* V1$_{Alpha}$-V5$_{Alpha}$ tACS can best be explained by reduced bottom-up V1 Alpha phase - V5 Gamma amplitude coupling (*ZPAC-V1p$_{Alpha}$V5a$_{Gamma}$*), and

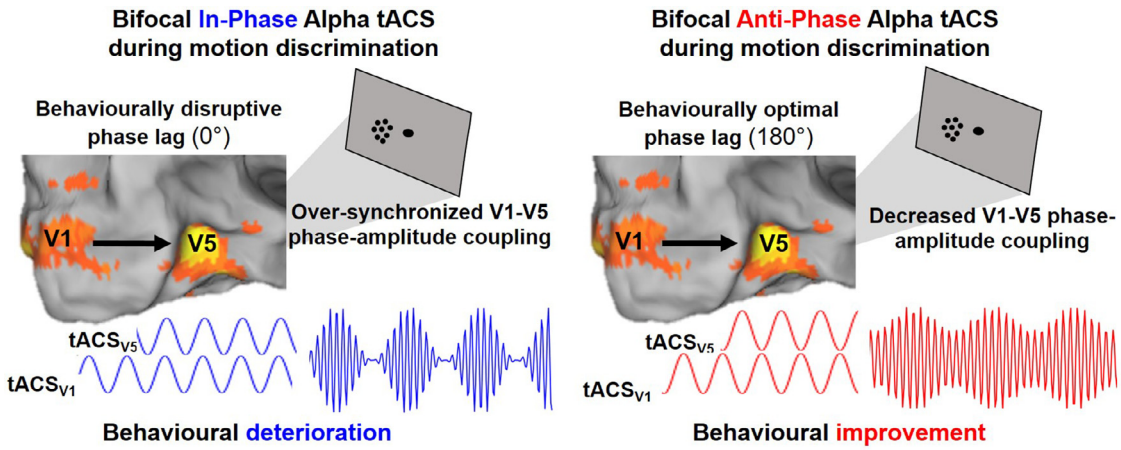

Fig. 5. Summary and mechanistic interpretation of the effects of bifocal In-Phase tACS (left part) and the Anti-Phase tACS (right part).

(3) the opposite, top-down modulation ($ZPAC\text{-}V5p_{Alpha}V1a_{Gamma}$) did not influence performance in the current paradigm.

4.1. Anti-Phase $V1A_{lpha}$-$V5_{Alpha}$ tACS and In-Phase $V1_{Alpha}$-$V5_{Alpha}$ tACS drive opposite effects on motion discrimination and integration

In-Phase tACS between two distant regions is motivated by the idea of increasing interregional synchronization and connectivity within a network (Polanía et al., 2012; Schwab et al., 2019; Vieira et al., 2020), under the hypothesis that a reduced phase-lag (~0°) between sites would promote an optimal inter-areal coupling and thus, optimal communication (Fries, 2005)). There is empirical evidence supporting this hypothesis. For instance, In-Phase stimulation has been associated with increased performance in visuo-attentional and memory tasks (Alagapan et al., 2019; Polanía et al., 2012; Violante et al., 2017), together with increased phase synchronization in the stimulated frequency band. In contrast to these data however, the present results showed opposite effects, i.e., the In-Phase condition rather impaired visual discrimination capacity during the stimulation period of 13±2 min, and performance did not improve, but rather decreased 10 and even 30 min after applying it.

Visual discrimination is associated with local Alpha desynchronization right after stimulus presentation (Dijk et al., 2008; Erickson et al., 2019; Hillyard et al., 1998; Sauseng et al., 2009; Zammit et al., 2018). Subsequently, it has been shown in several perceptual experimental modalities that a decrease in the Alpha-Beta band is linked to better stimulus perception (Griffiths et al., 2019). Thus, a high amplitude and zero-phase lag condition seems not to be optimal in this case because, as shown in the present data, focal increases in V1 Alpha phase - V5 Gamma amplitude coupling post stimulation (co-modulograms) are rather associated with poor performance. Instead, the underlying oscillatory mechanisms would most likely involve an intricate orchestration of oscillatory signatures that travels throughout the clusters of the neural network, controlled by stimuli properties (Muller et al., 2018). This oscillatory orchestration could be modeled as a multi-level interacting dynamical system (Alexander et al., 2019). Ultimately, cognition relies on feedback and feedforward dynamics. These processes are only possible through complex, well-orchestrated phase and amplitude interactions (Siegel et al., 2012).

From a more integrative perspective, the inhibition timing hypothesis (Klimesch, 2012) states that the optimal electrophysiological scenario that promotes perception relies on an inter-regional interplay of Alpha inhibition and Alpha disinhibition among areas belonging to the same network, as shown in the visual cortex (Shen et al., 2011). When this precise timing of activation/deactivation is disrupted by enforced Alpha In-Phase rhythms, it might generate a subsequent flood of massively synchronized signals, creating an artificial source of noise that may prevent accurate perception of stimulus features (Faisal et al., 2008; Voytek and Knight, 2015). The neuronal oscillatory system might require some time to come back to its basal processing state, as pointing to for the performance at 10 min and 30 min after stimulation of the In-Phase group.

In conclusion, though based on a straight forward assumption, positive behavioral effects are not always necessarily associated with an In-Phase synchronized magnification of the Alpha occipital rhythms, but under certain circumstances visual processing is driven through an ordered gating of oscillations that the Anti-Phase condition might promote. As a matter of fact, the improved offline performance reported in the present study is in accordance with a body of literature showing that inter-areal Anti-Phase stimulation might boost behavior in several contexts. For instance, Beta band Anti-Phase bi-hemispheric stimulation has been shown to increase visual attentional capacity (Yaple and Vakhrushev, 2018). In the same vein, Theta band Anti-Phase stimulation over the prefrontal and perysilvian area has been found to improve controlled memory retrieval (Marko et al., 2019), while Gamma band Anti-Phase stimulation between the cerebellum and M1 enhances visuomotor control (Miyaguchi et al., 2019). Here, we found that Anti-Phase $V1_{Alpha}$-$V5_{Alpha}$ tACS applied on average for 13±2 min during a motion discrimination task significantly supported motion direction discrimination and integration 10 min after the end of the stimulation and the effects continued to strengthen even 30 min later when compared to In-Phase.

Alekseichuk and colleagues compared intracranial recordings in the temporal area of macaques undergoing frontoparietal 10 Hz Anti-Phase or In-Phase stimulation, as well as, the voltage and electric field distribution associated with the two stimulation modes (Alekseichuk et al., 2019). Results showed a higher electric field magnitude, plus an unidirectional concentration of field lines for the Anti-Phase condition, whereas for the In-Phase condition there was a reduced magnitude and a bidirectional flow of electric field lines. The present electrical field simulation globally revealed similar spatial patterns suggesting that Anti-Phase stimulation generates more dynamical changes in electrical field distribution, with specific dynamics across time, which might be related to signal propagation speed.

After-effects of tACS are under debate in the field (Strüber et al., 2015), we think that the improved performance measured in the Anti-Phase group, which persists over time, are not only explained by an offline effect of the stimulation per se. Instead, we argue that it is the repeated practice of the task combined with the Anti-Phase tACS condition that promotes a "learning-like aftereffect". These after-effects might indeed find a justification in the accumulation of offline effects that lead to a carry-over of the achieved behavioral improvement (Heise et al., 2019). These offline effects might then generate favorable

plastic changes in the visual cortex due to the learning associated with the task, as it has been shown in non-human primates (Yang and Maunsell, 2004).

4.2. Anti-Phase tACS might exert its beneficial behavioural effects through bottom-up phase-amplitude decoupling

The present positive behavioral effects were associated with a bottom-up V1-Alpha phase V5-Gamma amplitude decoupling. This measure reflects the idea that the feedforward direction between V1 and V5 is regulated by a controlled amplitude modulation of Alpha-V1 over the phase of Gamma-V5, which scales with improved motion discrimination in the Anti-Phase group. Using EEG-derived phase amplitude coupling, it is possible to infer directionality of signal flow (Nandi et al., 2019). The direction of the coupling is assumed to be bottom-up if the modulating signal (Alpha band) is recorded in a primary functional neuronal population, located in lower anatomical areas (V1), whereas the carrier signal (Gamma band) is rather on higher cognitive and anatomical areas (MT/V5), receiving inputs mainly from other regions of the cortex (Jiang et al., 2015). Otherwise, the interaction ought to be top-down. This idea could be supported at some extent from a signal processing point of view, where it is presumed that in order to achieve modulation, the low frequency Alpha wave holding the information must travel and be imposed over the amplitude of the local high frequency Gamma that turns into the carrier wave (Roder, 1931). This superimposition of Alpha V1 into Gamma V5, provides a framework of direction and thus, an orientation of information flow. Furthermore, this idea is also fed by electrophysiological studies in primates, where it have been shown that high-frequency Gamma oscillatory activity (e.g., amplitude modulation coefficients almost equal to 1, meaning that the amplitude of the modulating signal equals the maximum peak amplitude of the carrier without modulation) preferably seems to travel in a feedforward manner in the visual cortex, whereas low-frequency Alpha (e.g., amplitude modulation coefficient almost equals to 0) appears to flow in a feedback direction (Michalareas et al., 2016) (van Kerkoerle et al., 2014).

Visual stimulus onset has been shown to trigger propagating rhythms in the primary and secondary visual cortices of monkeys, leading to a specific phase relationship between the oscillations at both sites (Muller et al., 2014). In humans, propagation of feedforward flows has been reported during visual motion discrimination, with latencies modulated by characteristics of the stimulus (Sato et al., 2012; Seriès et al., 2002). Then, this suggests the idea that there is an optimal range of Alpha rhythm magnitude that is more favorable to generate trains of local Gamma bursts, which might convey the most relevant information of the visual stimulus' features to promote motion discrimination (Nelli et al., 2017; Tu et al., 2016).

This bottom-up Alpha-Gamma interaction is in line with the theory of cross-frequency nested oscillations (Bonnefond et al., 2017). Accordingly, the organization of tasks in the visual system is done through the timed gating of information encoded in local Gamma bursts, happening every 10–30 ms and that are regulated through the Alpha inhibitory role (Jensen et al., 2014). Additionally, our finding that changes in phase amplitude coupling between Alpha-V1 and Gamma-V5 predict behavioural improvements in the Anti-Phase group is congruent with the fact that motion discrimination has been shown to occur as a feedforward oscillatory phenomenon (Seriès et al., 2002), and that these oscillations in the occipital cortex do not only belong to a single frequency band, but rather to a modulation of Alpha and Gamma rhythms (Bahramisharif et al., 2013).

Finally, we did not find any significant changes in the opposite top-down V5-Alpha phase - V1-Gamma Amplitude coupling and the values measured 10 min and 30 min after stimulation did not account for changes in motion discrimination performance or their variance. Although recordings in monkeys' visual cortex have shown a top-down Alpha-Beta that granger-causes a bottom-up Gamma rhythm (Richter et al., 2017), it does not necessarily contradict our findings since what we report reflect bottom-up coupled nested oscillations from one neuronal cluster to another, rather than a causal generation of oscillatory activity from one site to another. These markers indeed imply two different processes of interaction, in most of the circumstances, not mutually exclusive. Then, there might be different cross-frequency mechanisms that sustain visual discrimination that are revealed by these different electrophysiological markers. Exploring this variety of markers might lead to a better understanding of neural communication supporting visual discrimination.

5. Conclusions

The present experiments revealed that generating Anti-Phase oscillation patterns between V1 and V5 during motion discrimination using bi-focal tACS might enhance performance persisting even after the stimulation period. These after-effects were mechanistically partially explained by changes in bottom-up V1-Alpha V5-Gamma Phase-Amplitude coupling. We believe that these results might illustrate enhanced signal propagation from V1 to higher visual areas, under a precise phase-timing relationship. One can speculate that an optimal phase-lag between stimulation sites, induced by Anti-Phase tACS aftereffects, did promote neuronal communication because of the inherent speed of wave propagation. Furthermore, one could infer that Alpha Anti-Phase tACS might act as a controller of the Alpha disinhibition-gating capacities and as such, might modulate bottom-up trains of Gamma bursts in the V1-V5 pathway. The precise characteristics of the Gamma bursts (e.g., phase, time) might play a significant role in improving the performance in motion discrimination.

The present findings might point towards the exciting potential of the current approach to be extended towards an ameliorated stimulation orchestration with cross-frequency montages targeting the motion discrimination pathway. Furthermore, it potentially opens a novel direction of non-invasive interventions to treat patients with deficits in the visual domain, such as after a stroke.

6. Code and data availability

All codes and data used in the manuscript are available upon reasonable request addressed to the corresponding author.

Author contributions

Roberto F Salamanca-Giron: Methodology, Data curation, Software, Formal analysis, Resources, Writing – Original Draft; **Estelle Raffin:** Conceptualization, Data curation, Formal analysis, Supervision, Writing - review & editing, Funding acquisition; **Sarah B. Zandvliet:** Methodology, Writing - review & editing; Martin Seeber: Methodology, Writing and editing; **Christoph M. Michel:** Review and editing; **Paul Sauseng:** Methodology, Writing - review and editing; Krystel R. Huxlin: Conceptualization, Writing - review and editing; Friedhelm C. Hummel: Conceptualization, Supervision, Writing – review & editing, Supervision, Funding acquisition.

Declaration of Competing Interest

The authors declare no competing interests.

Acknowledgements

This research was funded by the Bertarelli Foundation (Catalyst BC77O7 to FCH & ER), by the Swiss National Science Foundation (PRIMA PR00P3_179867 to ER) and by the Defitech Foundation (to FCH).

Supplementary materials

Supplementary material associated with this article can be found, in the online version, at doi:10.1016/j.neuroimage.2021.118299.

References

Alagapan, S., Riddle, J., Huang, W.A., Hadar, E., Shin, H.W., Fröhlich, F., 2019. Network-targeted, multi-site direct cortical stimulation enhances working memory by modulating phase lag of low-frequency oscillations. Cell Rep. 29, 2590–2598. doi:10.1016/j.celrep.2019.10.072, e4.

Albright, et al., 1989. Centrifugal directional bias in the middle temporal visual area (MT) of the macaque. Vis. Neurosci. 2, 177–188. doi:10.1017/S0952523800012037.

Alekseichuk, I., Falchier, A.Y., Linn, G., Xu, T., Milham, M.P., Schroeder, C.E., Opitz, A., 2019. Electric field dynamics in the brain during multi-electrode transcranial electric stimulation. Nat. Commun. 10, 2573. doi:10.1038/s41467-019-10581-7.

Alexander, D.M., Ball, T., Schulze-Bonhage, A., Leeuwen, C.van, 2019. Large-scale cortical travelling waves predict localized future cortical signals. PLOS Comput. Biol. 15, e1007316. doi:10.1371/journal.pcbi.1007316.

Bahramisharif, A., Gerven, M.A.J., van, Aarnoutse, E.J., Mercier, M.R., Schwartz, T.H., Foxe, J.J., Ramsey, N.F., Jensen, O., 2013. Propagating neocortical gamma bursts are coordinated by traveling alpha waves. J. Neurosci. 33, 18849–18854. doi:10.1523/JNEUROSCI.2455-13.2013.

Bastos, A.M., Vezoli, J., Bosman, C.A., Schoffelen, J.-.M., Oostenveld, R., Dowdall, J.R., De Weerd, P., Kennedy, H., Fries, P., 2015. Visual areas exert feedforward and feedback influences through distinct frequency channels. Neuron 85, 390–401. doi:10.1016/j.neuron.2014.12.018.

Blakemore, C., Campbell, F.W., 1969. On the existence of neurones in the human visual system selectively sensitive to the orientation and size of retinal images. J. Physiol. 203, 237–260 1.

Bonnefond, M., Kastner, S., Jensen, O., 2017. Communication between brain areas based on nested oscillations. eNeuro 4. doi:10.1523/ENEURO.0153-16.2017.

Bosman, C.A., Schoffelen, J.-.M., Brunet, N., Oostenveld, R., Bastos, A.M., Womelsdorf, T., Rubehn, B., Stieglitz, T., De Weerd, P., Fries, P., 2012. Attentional stimulus selection through selective synchronization between monkey visual areas. Neuron 75, 875–888. doi:10.1016/j.neuron.2012.06.037.

Canolty, R.T., Edwards, E., Dalal, S.S., Soltani, M., Nagarajan, S.S., Kirsch, H.E., Berger, M.S., Barbaro, N.M., Knight, R.T., 2006. High gamma power is phase-locked to theta oscillations in human neocortex. Science 313, 1626–1628. doi:10.1126/science.1128115.

Carter, G.C., 1987. Coherence and time delay estimation. Proc. IEEE 75, 236–255. doi:10.1109/PROC.1987.13723.

Chouinard, P.A., Ivanowich, M., 2014. Is the primary visual cortex a center stage for the visual phenomenology of object size? J. Neurosci. 34, 2013–2014. doi:10.1523/JNEUROSCI.4902-13.2014.

Cohen, M.X., 2014. Analyzing Neural Time Series Data: Theory and Practice. MIT Press.

Cook, R.D., 1977. Detection of influential observation in linear regression. Technometrics 19, 15–18. doi:10.2307/1268249.

D'Agostino, R., Pearson, E.S., 1973. Tests for departure from normality. empirical results for the distributions of b2 and $\sqrt{b1}$. Biometrika 60, 613–622. doi:10.2307/2335012.

Das, A., Tadin, D., Huxlin, K.R., 2014. Beyond blindsight: properties of visual relearning in cortically blind fields. J. Neurosci. 34, 11652–11664. doi:10.1523/JNEUROSCI.1076-14.2014.

Dijk, H., van, Schoffelen, J.-.M., Oostenveld, R., Jensen, O., 2008. Prestimulus Oscillatory Activity in the Alpha Band Predicts Visual Discrimination Ability. J. Neurosci. 28, 1816–1823. doi:10.1523/JNEUROSCI.1853-07.2008.

Doesburg, S.M., Green, J.J., McDonald, J.J., Ward, L.M., 2009. From local inhibition to long-range integration: a functional dissociation of alpha-band synchronization across cortical scales in visuospatial attention. Brain Res 1303, 97–110. doi:10.1016/j.brainres.2009.09.069.

Doesburg, S.M., Green, J.J., McDonald, J.J., Ward, L.M., 2009. From local inhibition to long-range integration: a functional dissociation of alpha-band synchronization across cortical scales in visuospatial attention. Brain Res 1303, 97–110. doi:10.1016/j.brainres.2009.09.069.

Dosher, B.A., Lu, Z.L., 1998. Perceptual learning reflects external noise filtering and internal noise reduction through channel reweighting. Proc. Natl. Acad. Sci. 95, 13988–13993.

Elliott, M.A., Müller, H.J., 1998. Synchronous information presented in 40-HZ flicker enhances visual feature binding. Psychol. Sci. 9, 277–283. doi:10.1111/1467-9280.00055.

Engel, A.K., Kreiter, A.K., Konig, P., Singer, W., 1991. Synchronization of oscillatory neuronal responses between striate and extrastriate visual cortical areas of the cat. Proc. Natl. Acad. Sci. 88, 6048–6052. doi:10.1073/pnas.88.14.6048.

Erickson, M.A., Smith, D., Albrecht, M.A., Silverstein, S., 2019. Alpha-band desynchronization reflects memory-specific processes during visual change detection. Psychophysiology 56, e13442. doi:10.1111/psyp.13442.

Faisal, A.A., Selen, L.P.J., Wolpert, D.M., 2008. Noise in the nervous system. Nat. Rev. Neurosci. 9, 292–303. doi:10.1038/nrn2258.

Freunberger, R., Klimesch, W., Sauseng, P., Griesmayr, B., Höller, Y., Pecherstorfer, T., Hanslmayr, S., 2007. Gamma oscillatory activity in a visual discrimination task. Brain Res. Bull. 71, 593–600. doi:10.1016/j.brainresbull.2006.11.014.

Fries, P., 2015. Rhythms for cognition: communication through coherence. Neuron 88, 220–235. doi:10.1016/j.neuron.2015.09.034.

Fries, P., 2009. Neuronal gamma-band synchronization as a fundamental process in cortical computation. Annu. Rev. Neurosci. 32, 209–224. doi:10.1146/annurev.neuro.051508.135603.

Gangopadhyay, P., Chawla, M., Dal Monte, O., Chang, S.W.C., 2021. Prefrontal–amygdala circuits in social decision-making. Nat. Neurosci. 24, 5–18. doi:10.1038/s41593-020-00738-9.

Gilbert, C.D., Sigman, M., 2007. Brain States: Top-Down Influences in Sensory Processing. Neuron 54 (5), 677–696. doi:10.1016/j.neuron.2007.05.019.

Gilbert, C.D., Sigman, M., Crist, R.E., 2001. The Neural Basis of Perceptual Learning. Neuron 31, 681–697. doi:10.1016/S0896-6273(01)00424-X.

Gollo, L.L., Mirasso, C., Sporns, O., Breakspear, M., 2014. Mechanisms of zero-lag synchronization in cortical motifs. PLoS Comput. Biol. 10, e1003548. doi:10.1371/journal.pcbi.1003548.

Gramfort, A., Kowalski, M., Hämäläinen, M., 2012. Mixed-norm estimates for the M/EEG inverse problem using accelerated gradient methods. Phys. Med. Biol. 57, 1937–1961. doi:10.1088/0031-9155/57/7/1937.

Gramfort, A., Luessi, M., Larson, E., Engemann, D.A., Strohmeier, D., Brodbeck, C., Goj, R., Jas, M., Brooks, T., Parkkonen, L., Hämäläinen, M., 2013. MEG and EEG data analysis with MNE-Python. Front. Neurosci. 7. doi:10.3389/fnins.2013.00267.

Gray, C.M., Singer, W., 1989. Stimulus-specific neuronal oscillations in orientation columns of cat visual cortex. Proc. Natl. Acad. Sci. U. S. A. 86, 1698–1702.

Griffiths, B.J., Mayhew, S.D., Mullinger, K.J., Jorge, J., Charest, I., Wimber, M., Hanslmayr, S., 2019. Alpha/beta power decreases track the fidelity of stimulus-specific information. eLife 8, e49562. doi:10.7554/eLife.49562.

Hämäläinen, M.S., Ilmoniemi, R.J., 1994. Interpreting magnetic fields of the brain: minimum norm estimates. Med. Biol. Eng. Comput. 32, 35–42. doi:10.1007/BF02512476.

Heise, K.-.F., Monteiro, T.S., Leunissen, I., Mantini, D., Swinnen, S.P., 2019. Distinct online and offline effects of alpha and beta transcranial alternating current stimulation (tACS) on continuous bimanual performance and task-set switching. Sci. Rep. 9, 3144. doi:10.1038/s41598-019-39900-0.

Helfrich, R.F., Knepper, H., Nolte, G., Strüber, D., Rach, S., Herrmann, C.S., Schneider, T.R., Engel, A.K., 2014. Selective modulation of interhemispheric functional connectivity by HD-tACS shapes perception. PLoS Biol 12, e1002031. doi:10.1371/journal.pbio.1002031.

Hillyard, S.A., Teder-Sälejärvi, W.A., Münte, T.F., 1998. Temporal dynamics of early perceptual processing. Curr. Opin. Neurobiol. 8, 202–210. doi:10.1016/S0959-4388(98)80141-4.

Horovitz, S.G., Braun, A.R., Carr, W.S., Picchioni, D., Balkin, T.J., Fukunaga, M., Duyn, J.H., 2009. Decoupling of the brain's default mode network during deep sleep. Proc. Natl. Acad. Sci. U. S. A. 106, 11376–11381. doi:10.1073/pnas.0901435106.

Hülsdünker, T., Ostermann, M., Mierau, A., 2019. The Speed of Neural Visual Motion Perception and Processing Determines the Visuomotor Reaction Time of Young Elite Table Tennis Athletes.. Front. Behav. Neurosci. 13, 165. doi:10.3389/fnbeh.2019.00165.

Huxlin, K.R., Martin, T., Kelly, K., Riley, M., Friedman, D.I., Burgin, W.S., Hayhoe, M., 2009. Perceptual relearning of complex visual motion after V1 damage in Humans. J. Neurosci. 29, 3981–3991. doi:10.1523/JNEUROSCI.4882-08.2009.

Jensen, O., Gips, B., Bergmann, T.O., Bonnefond, M., 2014. Temporal coding organized by coupled alpha and gamma oscillations prioritize visual processing. Trends Neurosci 37, 357–369. doi:10.1016/j.tins.2014.04.001.

Jia, X., Tanabe, S., Kohn, A., 2013. Gamma and the Coordination of Spiking Activity in Early Visual Cortex. Neuron 77, 762–774. doi:10.1016/j.neuron.2012.12.036.

Jiang, H., Bahramisharif, A., van Gerven, M.A.J., Jensen, O., 2015. Measuring directionality between neuronal oscillations of different frequencies. NeuroImage 118, 359–367. doi:10.1016/j.neuroimage.2015.05.044.

Kar, K., Krekelberg, B., 2014. Transcranial Alternating Current Stimulation Attenuates Visual Motion Adaptation. J. Neurosci 34, 7334–7340.

Klimesch, W., 2012. Alpha-band oscillations, attention, and controlled access to stored information. Trends Cogn. Sci. 16, 606–617. doi:10.1016/j.tics.2012.10.007.

Lamme, V.A.F., Roelfsema, P.R., 2000. The distinct modes of vision offered by feedforward and recurrent processing. Trends Neurosci 23, 571–579. doi:10.1016/S0166-2236(00)01657-X.

Lewis, C.M., Bosman, C.A., Womelsdorf, T., Fries, P., 2016. Stimulus-induced visual cortical networks are recapitulated by spontaneous local and interareal synchronization. Proc. Natl. Acad. Sci. U. S. A. 113, E606–E615. doi:10.1073/pnas.1513773113.

Lin, F.-.H., Belliveau, J.W., Dale, A.M., Hämäläinen, M.S., 2006. Distributed current estimates using cortical orientation constraints. Hum. Brain Mapp. 27, 1–13. doi:10.1002/hbm.20155.

Marko, M., Cimrová, B., Riečanský, I., 2019. Neural theta oscillations support semantic memory retrieval. Sci. Rep. 9, 17667. doi:10.1038/s41598-019-53813-y.

Michalareas, G., Vezoli, J., van Pelt, S., Schoffelen, J.-.M., Kennedy, H., Fries, P., 2016. Alpha-Beta and gamma rhythms subserve feedback and feedforward influences among human visual cortical areas. Neuron 89, 384–397. doi:10.1016/j.neuron.2015.12.018.

Miyaguchi, S., Otsuru, N., Kojima, S., Yokota, H., Saito, K., Inukai, Y., Onishi, H., 2019. Gamma tACS over M1 and cerebellar hemisphere improves motor performance in a phase-specific manner. Neurosci. Lett. 694, 64–68. doi:10.1016/j.neulet.2018.11.015.

Muller, L., Chavane, F., Reynolds, J., Sejnowski, T.J., 2018. Cortical travelling waves: mechanisms and computational principles. Nat. Rev. Neurosci. 19, 255–268. doi:10.1038/nrn.2018.20.

Muller, L., Reynaud, A., Chavane, F., Destexhe, A., 2014. The stimulus-evoked population response in visual cortex of awake monkey is a propagating wave. Nat. Commun. 5. doi:10.1038/ncomms4675.

Nandi, B., Swiatek, P., Kocsis, B., Ding, M., 2019. Inferring the direction of rhythmic neural transmission via inter-regional phase-amplitude coupling (ir-PAC). Sci. Rep. 9, 6933. doi:10.1038/s41598-019-43272-w.

Nelli, S., Itthipuripat, S., Srinivasan, R., Serences, J.T., 2017. Fluctuations in instantaneous frequency predict alpha amplitude during visual perception. Nat. Commun. 8, 2071. doi:10.1038/s41467-017-02176-x.

Neuling, T., Rach, S., Hermann, C.S., 2013. Orchestrating neuronal networks: sustained after-effects of transcranial alternating current stimulation depend upon brain states. Front. Hum. Neurosci. 7. doi:10.3389/fnhum.2013.00161.

Newsome, W., Pare, E., 1988. A selective impairment of motion perception following lesions of the middle temporal visual area (MT). J. Neurosci. 8, 2201–2211. doi:10.1523/JNEUROSCI.08-06-02201.1988.

Nowak, L.G., Sanchez-Vives, M.V., McCormick, D.A., 2008. Lack of orientation and direction selectivity in a subgroup of fast-spiking inhibitory interneurons: cellular and synaptic mechanisms and comparison with other electrophysiological cell types. Cereb. Cortex N. Y. N 18, 1058–1078. doi:10.1093/cercor/bhm137, 1991.

Oemisch, M., Westendorff, S., Everling, S., Womelsdorf, T., 2015. Interareal spike-train correlations of anterior cingulate and dorsal prefrontal cortex during attention shifts. J. Neurosci. 35, 13076–13089. doi:10.1523/JNEUROSCI.1262-15.2015.

Palva, J.M., Wang, S.H., Palva, S., Zhigalov, A., Monto, S., Brookes, M.J., Schoffelen, J.-M., Jerbi, K., 2018. Ghost interactions in MEG/EEG source space: a note of caution on inter-areal coupling measures. NeuroImage 173, 632–643. doi:10.1016/j.neuroimage.2018.02.032.

Palva, S., Palva, J.M., 2011. Functional roles of alpha-band phase synchronization in local and large-scale cortical networks. Front. Psychol. 2. doi:10.3389/fpsyg.2011.00204.

Petkoski, S., Jirsa, V.K., 2019. Transmission time delays organize the brain network synchronization. Philos. Transact. A Math. Phys. Eng. Sci. 377. doi:10.1098/rsta.2018.0132.

Polanía, R., Nitsche, M.A., Korman, C., Batsikadze, G., Paulus, W., 2012. The importance of timing in segregated theta phase-coupling for cognitive performance. Curr. Biol. 22, 1314–1318. doi:10.1016/j.cub.2012.05.021.

Pooresmaeili, A., Poort, J., Roelfsema, P.R., 2014. Simultaneous selection by object-based attention in visual and frontal cortex. Proc. Natl. Acad. Sci. 111, 6467–6472. doi:10.1073/pnas.1316181111.

Richter, C.G., Thompson, W.H., Bosman, C.A., Fries, P., 2017. Top-down beta enhances bottom-up gamma. J. Neurosci. Off. J. Soc. Neurosci. 37, 6698–6711. doi:10.1523/JNEUROSCI.3771-16.2017.

Roberts, M.J., Lowet, E., Brunet, N.M., Ter Wal, M., Tiesinga, P., Fries, P., De Weerd, P., 2013. Robust gamma coherence between macaque V1 and V2 by dynamic frequency matching. Neuron 78, 523–536. doi:10.1016/j.neuron.2013.03.003.

Roe, A.W., Ts'o, D.Y., 1999. Specificity of color connectivity between primate V1 and V2. J. Neurophysiol. 82, 2719–2730. doi:10.1152/jn.1999.82.5.2719.

Roelfsema, P.R., Engel, A.K., König, P., Singer, W., 1997. Visuomotor integration is associated with zero time-lag synchronization among cortical areas. Nature 385, 157–161. doi:10.1038/385157a0.

Ruff, D.A., Cohen, M.R., 2016. Attention increases spike count correlations between visual cortical areas. J. Neurosci. 36, 7523–7534. doi:10.1523/JNEUROSCI.0610-16.2016.

Salazar, R., Dotson, N., Bressler, S., Gray, C., 2012. Content specific fronto-parietal synchronization during visual working memory. Science 338, 1097–1100. doi:10.1126/science.1224000.

Sato, T.K., Nauhaus, I., Carandini, M., 2012. Traveling waves in visual cortex. Neuron 75, 218–229. doi:10.1016/j.neuron.2012.06.029.

Saturnino, G.B., Madsen, K.H., Siebner, H.R., Thielscher, A., 2017. How to target inter-regional phase synchronization with dual-site Transcranial Alternating Current Stimulation. NeuroImage 163, 68–80. doi:10.1016/j.neuroimage.2017.09.024.

Sauseng, P., Klimesch, W., Heise, K.F., Gruber, W.R., Holz, E., Karim, A.A., Glennon, M., Gerloff, C., Birbaumer, N., Hummel, F.C., 2009. Brain oscillatory substrates of visual short-term memory capacity. Curr. Biol. CB 19, 1846–1852. doi:10.1016/j.cub.2009.08.062.

Schipul, S.E., Keller, T.A., Just, M.A., 2011. Inter-regional brain communication and its disturbance in autism. Front. Syst. Neurosci. 5, 10. doi:10.3389/fnsys.2011.00010.

Schwab, B.C., Misselhorn, J., Engel, A.K., 2019. Modulation of large-scale cortical coupling by transcranial alternating current stimulation. Brain Stimul. Basic Transl. Clin. Res. Neuromodulation 12, 1187–1196. doi:10.1016/j.brs.2019.04.013.

Seiffert, A., Somers, D., Dale, A., Tootell, R., 2003. Functional MRI studies of human visual motion perception: texture, luminance, attention and after-effects. Cereb Cortex 13, 340–349.

Semedo, J.D., Zandvakili, A., Machens, C.K., Yu, B.M., Kohn, A., 2019. Cortical areas interact through a communication subspace. Neuron 102, 249–259. doi:10.1016/j.neuron.2019.01.026, e4.

Seriès, P., Georges, S., Lorenceau, J., Frégnac, Y., 2002. Orientation dependent modulation of apparent speed: a model based on the dynamics of feed-forward and horizontal connectivity in V1 cortex. Vision Res 42, 2781–2797. doi:10.1016/s0042-6989(02)00302-4.

Seymour, R.A., Rippon, G., Gooding-Williams, G., Schoffelen, J.M., Kessler, K., 2019. Dysregulated oscillatory connectivity in the visual system in autism spectrum disorder. Brain 142, 3294–3305. doi:10.1093/brain/awz214.

Shen, W., McKeown, C.R., Demas, J.A., Cline, H.T., 2011. Inhibition to excitation ratio regulates visual system responses and behavior *in vivo*. J. Neurophysiol. 106, 2285–2302. doi:10.1152/jn.00641.2011.

Siegel, M., Donner, T.H., Engel, A.K., 2012. Spectral fingerprints of large-scale neuronal interactions. Nat. Rev. Neurosci. 13, 121–134. doi:10.1038/nrn3137.

Siegel, M., Donner, T.H., Oostenveld, R., Fries, P., Engel, A.K., 2008. Neuronal synchronization along the dorsal visual pathway reflects the focus of spatial attention. Neuron 60, 709–719. doi:10.1016/j.neuron.2008.09.010.

Siegel, M., Donner, T.H., Oostenveld, R., Fries, P., Engel, A.K., 2007. High-frequency activity in human visual cortex is modulated by visual motion strength. Cereb. Cortex 17, 732–741. doi:10.1093/cercor/bhk025.

Simoncelli, E.P., Heeger, D.J., 1998. A model of neuronal responses in visual area MT. Vision Res 38, 743–761. doi:10.1016/s0042-6989(97)00183-1.

Strüber, D., Rach, S., Neuling, T., Herrmann, C.S., 2015. On the possible role of stimulation duration for after-effects of transcranial alternating current stimulation. Front. Cell. Neurosci. 9. doi:10.3389/fncel.2015.00311.

Thielscher, A., Antunes, A., Saturnino, G.B., 2015. Field modeling for transcranial magnetic stimulation: a useful tool to understand the physiological effects of TMS? In: Proceedings of the 37th Annual International Conference of the IEEE Engineering in Medicine and Biology Society (EMBC). 37th Annual International Conference of the IEEE Engineering in Medicine and Biology Society (EMBC), Milan. IEEE, pp. 222–225. doi:10.1109/EMBC.2015.7318340.

Tibshirani, R., 1996. Regression shrinkage and selection via the Lasso. J. R. Stat. Soc. Ser. B Methodol. 58, 267–288.

Townsend, R.G., Solomon, S.S., Martin, P.R., Solomon, S.G., Gong, P., 2017. Visual motion discrimination by propagating patterns in primate cerebral cortex. J. Neurosci. 37, 10074–10084. doi:10.1523/JNEUROSCI.1538-17.2017.

Tu, Y., Zhang, Z., Tan, A., Peng, W., Hung, Y.S., Moayedi, M., Iannetti, G.D., Hu, L., 2016. Alpha and gamma oscillation amplitudes synergistically predict the perception of forthcoming nociceptive stimuli. Hum. Brain Mapp. 37, 501–514. doi:10.1002/hbm.23048.

van Kerkoerle, T., Self, M.W., Damino, B., Gariel-Mathis, M.-A., Poort, J., van der Togt, C., Roelfsema, P.R., 2014. Alpha and gamma oscillations characterize feedback and feedforward processing in monkey visual cortex. Proc. Natl. Acad. Sci. 111, 14332–14341. doi:10.1073/pnas.1402773111.

Vieira, P.G., Krause, M.R., Pack, C.C., 2020. tACS entrains neural activity while somatosensory input is blocked. PLOS Biol 18, e3000834. doi:10.1371/journal.pbio.3000834.

Violante, I.R., Li, L.M., Carmichael, D.W., Lorenz, R., Leech, R., Hampshire, A., Rothwell, J.C., Sharp, D.J., 2017. Externally induced frontoparietal synchronization modulates network dynamics and enhances working memory performance. eLife 6, e22001. doi:10.7554/eLife.22001.

von Stein, A., Chiang, C., König, P., 2000. Top-down processing mediated by interareal synchronization. Proc. Natl. Acad. Sci. U. S. A. 97, 14748–14753.

Vosskuhl, J., Huster, R.J., Herrmann, C.S., 2016. BOLD signal effects of transcranial alternating current stimulation (tACS) in the alpha range: A concurrent tACS-fMRI study. Neuroimage 140, 118–125.

Voytek, B., Knight, R.T., 2015. Dynamic network communication as a unifying neural basis for cognition, development, aging, and disease. Biol. Psychiatry 77, 1089–1097. doi:10.1016/j.biopsych.2015.04.016.

Wakeman, D.G., Henson, R.N., 2015. A multi-subject, multi-modal human neuroimaging dataset. Sci. Data 2, 150001. doi:10.1038/sdata.2015.1.

Wang, J., Brown, R., Dobkins, K.R., McDowell, J.E., Clementz, B.A., 2010. Diminished parietal cortex activity associated with poor motion direction discrimination performance in schizophrenia. Cereb. Cortex 20, 1749–1755. doi:10.1093/cercor/bhp243.

Welch, P., 1967. The use of fast Fourier transform for the estimation of power spectra: a method based on time averaging over short, modified periodograms. IEEE Trans. Audio Electroacoustics 15, 70–73. doi:10.1109/TAU.1967.1161901.

Wen, T., Liu, D.-C., Hsieh, S., 2018. Connectivity patterns in cognitive control networks predict naturalistic multitasking ability. Neuropsychologia 114, 195–202. doi:10.1016/j.neuropsychologia.2018.05.002.

Yang, T., Maunsell, J.H.R., 2004. The effect of perceptual learning on neuronal responses in monkey visual area V4. J. Neurosci. Off. J. Soc. Neurosci. 24, 1617–1626. doi:10.1523/JNEUROSCI.4442-03.2004.

Yaple, Z., Vakhrushev, R., 2018. Modulation of the frontal-parietal network by low intensity anti-phase 20 Hz transcranial electrical stimulation boosts performance in the attentional blink task. Int. J. Psychophysiol. Off. J. Int. Organ. Psychophysiol. 127, 11–16. doi:10.1016/j.ijpsycho.2018.02.014.

Zaehle, T., Rach, S., Herrmann, C.S., 2010. Transcranial Alternating Current Stimulation Enhances Individual Alpha Activity in Human EEG. Plos One 5 (11). doi:10.1371/journal.pone.0013766.

Zammit, N., Falzon, O., Camilleri, K., Muscat, R., 2018. Working memory alpha-beta band oscillatory signatures in adolescents and young adults. Eur. J. Neurosci. 48, 2527–2536. doi:10.1111/ejn.13897.

Zhang, H., Morrone, M.C., Alais, D., 2019. Behavioural oscillations in visual orientation discrimination reveal distinct modulation rates for both sensitivity and response bias. Sci. Rep. 9, 1115. doi:10.1038/s41598-018-37918-4.

Zito, G.A., Senti, T., Cazzoli, D., Müri, R.M., Mosimann, U.P., Nyffeler, T., Nef, T., 2015. Cathodal HD-tDCS on the right V5 improves motion perception in human. Front. Behav. neurosci. 9. doi:10.3389/fnbeh.2015.00257.